EFDA–JET–CP(07)06-07

T. Johnson, J. Lönnroth, P.C. de Vries, A. Salmi, L.-G. Eriksson, V. Hynönen,
I. Jenkins, J. Ongena, N. Oyama, V. Parail, G. Saibene, S. Sharapov,
K. Shinohara and JET-EFDA contributors

HALEKAR Modelling of Fast Particle Transport and Losses with TF Ripple in JET

HALEKAR Modelling of Fast Particle Transport and Losses with TF Ripple in JET

T. Johnson[1], J. Lönnroth[2], P. C. de Vries[3], A. Salmi[2], L.-G. Eriksson[4], V. Hynönen[2], I. Jenkins[3], J. Ongena[5], N. Oyama[6], V. Parail[3], G. Saibene[7], S. Sharapov[3], K. Shinohara[6] and JET-EFDA contributors*

JET-EFDA, Culham Science Centre, OX14 3DB, Abingdon, UK

[1]EURATOM-VR Association, Fusion Plasma Physics, EES, KTH , 10044 Stockholm, Sweden
[2]Helsinki University of Technology, Association Euratom-Tekes, FI-02015 TKK, Finland
[3]EURATOM /UKAEA Fusion Association, Culham Science Centre, Abingdon, OX14 3DB, UK
[4]Assoiation EURATOM/CEA, Cadarache, France
[5]Plasma Physics Laboratory, Royal Military Academy, Association EUROATOM – Belgian State, Bryssels, Belgium
[6]JAEA Naka, Ibaraki-ken, 311-0193 Japan
[7]EFDA CSU-Garching, Germany
** See annex of M.L. Watkins et al, "Overview of JET Results ",*
(Proc. 21 st IAEA Fusion Energy Conference, Chengdu, China (2006)).

Preprint of Paper to be submitted for publication in Proceedings of the
10th IAEA Technical Meeting on Energetic Particles in Magnetic Confinement Systems,
Kloster Seeon, Germany.
(8th October 2007 - 10th October 2007)

ABSTRACT.
In preparation for ripple experiments at JET the heat loads from fast ions to plasma facing components were calculated by orbit following Monte Carlo codes. The calculations show that losses are generated by two mechanisms, ripple-trapping and ripple-banana diffusion, and that the heat loads could cause damage to plasma facing components. During the experiments the auxiliary power was therefore kept below the limits inferred from the simulations. Measurements of the losses of fast ions from NBI using visible-light and infrared cameras have been shown to be in agreement with the predictions from the simulations. Finally, interactions between fast ions and the non-axisymmetric magnetic field are shown to generate a toroidal torque, which in JET with ~1% ripple is of the same order as that from neutral beam injection.

1. INTRODUCTION

In tokamak devices the finite number of Toroidal Field (TF) coils causes a toroidal variation of the magnetic field; called ripple. The ripple breaks the toroidal symmetry of the tokamak, thus introducing a transport channel that constrains the design of a tokamak reactors; the ripple must be low enough to both allow confinement of alpha particles and to avoid high heat fluxes to the Plasma Facing Components (PFC). In JET the 32 TF coils can be configured such that the odd and the even numbered coils carry different currents, thus allowing for external control of the ripple amplitude. In early 2007 a set of experiments were performed to study the impact of ripple on JET plasmas. In preparation for the experiments a modelling project was launched to find an operational space for NBI and ICRH with respect to ripple-induced ion losses to PFC, and for predictions of the plasma performance. The project focused on simulations with the Monte Carlo codes OFMC, ASCOT and SELFO.

The TF ripple amplitude, $\delta\,(R,Z) = [B_{max}(R,Z) - B_{min}\,(R,Z)] / [B_{max}\,(R,Z) + B_{min}\,(R,Z)]$, depends strongly (approximately exponentially) on the ratio between the distance from (R,Z) to the TF coils-system and the distance between two coils. Here B_{max} and B_{min} are the maximum and minimum magnetic field along the circle for which the major radius R and the vertical coordinate Z are constant. The ripple amplitude can therefore differ by several orders of magnitude between the plasma core and edge. Furthermore, the distance between TF coils is larger on the outboard, than the inboard side. The highest ripple inside the plasma is therefore often found at the separatrix near the outboard equatorial plane. Values quoted in this paper are taken at R = 3.80m, Z = 0m, which is close to this maximum. In standard operation with 32 coils this amplitude is 0.08%, while when the ratio of the currents in odd and even coils are 0.33, 0.5 and 0.66, the ripple amplitudes are 0.5%, 1% and 1.5%, respectively.

2. TRANSPORT AND LOSSES INDUCED BY TF RIPPLE

The toroidal field ripple enhances the transport of fast ions by modifying their guiding centre orbit. This transport can be separated into two mechanisms: ripple-trapped transport and ripple-banana diffusion. The latter appears due to the ripple induced perturbation of the magnetic field strength around the turning points of a banana-orbit. If the ripple enhances the local magnetic field, then the

ion will reach the turning point earlier and the accumulated grad-B and curvature drifts are reduced, resulting in a radial displacement of the orbit; see figure 1. When successive radial displacements are decorrelated, e.g. by collision, wave interaction, or intrinsic stochastisity, a diffusive type of transport is obtained which we will call 'ripple-banana diffusion' [1].

Ripple-trapped transport appears when particles become trapped in the magnetic wells appearing in between the Toroidal Field (TF) coils [2]. These 'ripple-trapped' ions will move in the poloidal plane through grad-B and curvature drifts; for standard JET operation the current and magnetic field direction is clockwise when viewed from above yielding a downward drift. This is of particular concern for ripple operation in JET since it allows energetic ions to reach deep in between poloidal limiters where sensitive Plasma Facing Components (PFC) are located. The most sensitive components are a TAE antenna, which can sustain 150-200 kW/m^2 of ripple-trapped losses, and pipes called 'French horns' that supply the divertor region with cooling water.

Banana orbits that are transported out of the plasma by ripple-banana diffusion are usually scraped of by the PFC closest to the plasma; in JET this means the poloidal limiters, or the divertor. However, a smaller number of fast ions manage to reach the more sensitive Faraday screens in front of the ICRH antennas, which can take losses up to 1 MW/m^2. In order not to damage the Faraday screen the loads on the poloidal limiters have to be less than approximately 7 MW/m^2. This constraint has been used as the operations limit for ripple-banana losses.

3. SIMULATION TOOLS

To estimate the losses of fast ions to PFC's with enhanced TF ripple in JET numerical simulation have been performed using the three Monte Carlo codes OFMC, ASCOT and SELFO. The OFMC code (from JAEA) [3-5] have been used to simulate neutral beam injection by follow the guiding centres of a set of test particles, representing the beam ions, as they slow down and scatter through collisions with a Maxwellian background plasma. In OFMC the simulation domain is bounded by a wall, representing the PFC. This wall includes representations of the poloidal limiters and the ICRH and the LHCD antennas, onto which heat loads can be evaluated; see figure 2. Like OFMC, the ASCOT code [6-9] is a guiding following Monte Carlo code. It has been used to trace both beam ions and ICRH accelerated ions. In addition to providing information about the fast ion losses, ASCOT has also been used to evaluate the torques delivered by NBI ions in the presence of ripple, as described in section 7.

SELFO [10] is an orbit averaged Monte Carlo code for ICRH modelling. Although SELFO does not include effects from ripple, it has been used to calculate steady state distribution functions of ICRF accelerated ions in absence of ripple. Test particles from the steady state distribution are then used as input in ASCOT, which calculates the losses due to ripple by tracing their orbits in a non-axisymmetric field during collisional slowing down and scattering. This approached is based on the assumption that most ions that are strongly affected by the ripple have their turning points on the low field side of the cyclotron resonance and do not resonate with the ICRF waves. The assumption is, at least partially, validated by the very low ripple along and on the high field side of the resonance.

4. SIMULATION RESULTS FOR NEUTRAL BEAM INJECTION

Modelling of neutral beam heating and the associated fast ion losses have been performed for a large number of plasmas. The main purpose of the simulations was to estimate the heat loads on PFC in order to assure machine safety. But the results were also of use when planning the experiments by e.g. providing values for the reduction in heating efficiency from ripple losses.

The modelling suggests that ripple losses of beam ions can cause significant damage to PFC if the maximum available power is applied. E.g. at 0.5% ripple an NBI power of 20 MW may be acceptable, while for similar plasmas at 1.5% ripple the power should restricted to be less than 7 MW for safe operation. The exact values of the operational boundaries depends not only on the ripple amplitude, but also on the plasma shape and on plasma parameters; at higher density more beam ions are born near the plasma edge where the ripple is high, while higher plasma current improves the fast ion confinement and reduces the size of the ripple wells. Attempts have been made to derive scaling laws from the results of the OFMC predictions, but the losses proved to have a too complex dependence on too many parameters for such a scaling law to be accurate.

From analysis of the results of the simulations emerged the following picture of the physical process driving the losses. In JET beam ions that are born close to the plasma edge will follow trapped banana orbits with their turning points outside the ripple-well region; thus they are susceptible to ripple-banana diffusion, but not ripple trapping. These ions will initially collide mainly with the electrons, generating a steady slowing down, but as their energy decreases the pitch-angle scattering becomes stronger. In those parts of the plasma where there are ripple wells the pitch angle scattering provides a supply of ripple-trapped ions. Thus, losses of beam ions are caused by both ripple-banana diffusion and from ripple trapping. While ripple-banana diffusion can lead to losses at energies close to the injection energy, the ions lost through ripple trapping are in general less energetic.

The relative importance of ripple trapped and ripple-banana losses is mainly determined by the size of the regions with ripple wells; due to the short time scale needed for a ripple-trapped ion to be lost the ratio of ripple-trapped to banana losses increases with the ripple amplitude. In fact, for 1.5% ripple the operational boundaries were in general set by ripple trapped losses, while 0.5% ripple the ripple-banana losses set the operational boundaries.

Figure 2 shows an illustration of how the losses are distributed to PFC. Here the ripple-trapped losses can be found around poloidal angles -65^{O}, about 0.5 m below the equatorial plane, and ripple-banana losses are found on the poloidal limiters slightly below the equatorial plane (poloidal angle 0^{o}). To be more precise, the ripple-banana losses appear on the left edge of the poloidal limiters; as the toroidal velocity on the outer leg of banana orbits is along the plasma current (in the figure 2 the plasma current flows from left to right).

5. RIPPLE LOSSES OF ICRF ACCELERATED IONS

In JET heating by ICRF waves can accelerate populations of fast ion with energies between hundreds of keV to a few MeV. Since this acceleration is mainly perpendicular to the magnetic field and the

slowing down is weak, the distribution functions of the fast ions become dominated by banana-trapped ions with their turning points around the cyclotron resonance layer. To avoid that these poloidally trapped ions become ripple-trapped the cyclotron resonance layer have to be kept far away from the ripple-well region [11]. Therefore, for operation with TF ripple in JET the ICRF system was only allowed to operate with an on-axis of slightly Low Field Side (LFS) resonance. Consequently, ripple trapped losses are very rare in all simulations of ICRH losses with ripple.

Furthermore, operation with LFS, or on-axis, cyclotron resonance means that the ripple levels around the resonance layer are generally small. Still, ripple-banana diffusion can significantly contribute to the losses of ions with MeV energies. Since these ions usually appear in the tail of an approximately exponential distribution function, the heat loads from ICRF accelerated ions will depend non-linearly on the average energy of the fast ions, and consequently on the ICRF power absorbed per resonant ion.

An issue of great concern for operation with ICRH at high ripple is that the accelerated ions are prone to drive global MHD modes, which in turn can transport the fast ions into the ripple-well region and indirectly cause ripple-trapped losses. As reported in Ref. [12] such losses are believed to be responsible for having caused damage to PFC in TFTR. Although analysis showed that these losses are less likely in JET, it was decided that high amplitude global MHD modes should be avoided. Consequently, the ICRH power was kept low during the ripple experiments and the losses predicted by modelling were typically an order of magnitude below the safety margin. Thus, neither the visible-light, nor the IR cameras were able to detect the ICRF induced losses.

6. EXPERIMENTAL OBSERVATIONS

The question arises if the predictions of the Monte Carlo calculations can be verified by measurements and observations. Although ripple trapped losses have been detected by fast ion diagnostics [13], direct comparison with the predicted heat loads are not available. However, visual inspection of the TAE antenna after the ripple experiments were performed confirms that ripple losses did not cause any damage to the antenna. We believe that damage could appear for losses of about twice the maximum Monte Carlo predictions. Thus, we deduce that the simulation did not give a strong underestimation of the maximum ripple-trapped losses.

Direct evidence of losses due to ripple-banana diffusion was found with the visible-light and IR camera [14-15]. In figure 3 an example is shown of two discharge, one with an enhance TF ripple of 1% and the other with the standard JET 32 coils ripple (0.08 %). OFMC simulations for the 1% ripple pulse predicts that heat loads of approximately 4.6 MW/m^2 are deposited on the poloidal limiter at a location that is in good agreement with the bright spots seen on the poloidal limiter. Furthermore, when changing the plasma scenario or the plasma shape the bright spots appear at different locations on the poloidal limiters. These variations are in agreement with OFMC simulations.

A strong indication of a correlation between the prediction and the experimental losses are obtained from studying the threshold for bright spots to be visible with the visible-light camera. For pulses

where OFMC predicts a heat load less than 3.3 MW there are no visible loads observed, while when the prediction is larger than 4.3 MW bright spots are always observed.

As an example, for neutral injection along beam lines that are tangential to the flux surfaces at ~1.85 m there is significantly less losses than for more perpendicular injection with a tangency radius of ~1.3 m. For one particular type H-mode plasma OFMC predicted 2.8 MW/m^2 and 4.3 MW/m^2 for the two NBI configurations, respectively. In the experiments bright spots were observed for the more perpendicular injection, but not for the more parallel injection.

Measurements with the IR camera allow for direct comparison with the predicted heat loads. The IR camera measures local temperatures of the PFC. Under assumptions that a heat load, Q, is applied at time t=0 the temperature evolution can be approximated by

$$T(t) = Q\sqrt{t}/k, \qquad (1)$$

where $k = \sqrt{\pi\lambda c\rho}/4$, for which λ, ρ and c are the thermal conductivity, the density and heat capacity of the material (for the JET tiles of interest k~18400Wm^{-2}s$^{1/2}$). By matching the time dependence of the measured limiter temperatures to Eq. (1) the heat loads can be estimated. The result, illustrated in figure 4, is that the reconstructed heat loads that are close to those predicted by the Monte Carlo simulations.

There are a number of sources for errors in the estimated heat loads, e.g. from the assumptions underlying Eq. (1), from matching the measured temperatures to this equation, from the uncertainties in the value of k, from errors in the IR measurements of the surface temperature and from systematic errors in the measurements. One systematic error is obtained from the fact that the IR cannot see the parts of the limiters where the highest losses are expected; before being lost, the ions travel towards the camera and are therefore most likely to hit the shadow side of the limiters. However, due to thermal conduction the observed temperatures should be close to the maximum temperature.

There are also errors in the predicted heat loads. The predictions are based on test particles simulations with a statistical error. Since the quantity of interest is the maximum heat load the statistical error may enhance the prediction. Furthermore, some of the simulations used in generating figure 4 were performed with a beam line geometry that was different from what was used in the experiment. This may result in additional scatter of the data.

7. RIPPLE AND PLASMA ROTATION

Fast ions that are transported by TF ripple do so by receiving toroidal momentum from the magnetic field through $v \times B$ forces. The connection between radial transport of trapped orbits and toroidal momentum can be found in the form of the canonical toroidal angular momentum, $P_\phi = Ze\psi + Rmv_\phi$, where Ze and m are the ion charge and mass, v_ϕ is the toroidal velocity, R is the major radius and ψ is the poloidal magnetic flux normalised by 2π. In general ripple perturbation of ion orbits are adiabatic and P_ϕ oscillates adiabatically. However, near the turning points the phase of the ripple becomes

stationary and a net toroidal momentum is transferred to the ion, thus changing v_ϕ and consequently P_ϕ. Since the flux surface at the turning point ($v_\phi = 0$) is given by $\psi = P_\phi/Ze$, the ripple has caused radial transport.

The torque that the fast ion receive from the non-axissymetric magnetic field, $\boldsymbol{\tau}$, is thus transferred into a radial current $j_\phi = -\boldsymbol{\tau}/RB_p$, where B_p is the poloidal magnetic field. To maintain quasi-neutrality the background plasma sets up a return current $j_r = -j_\phi$, which generates a torque $R\boldsymbol{j}_r \times \boldsymbol{B}_p = \boldsymbol{\tau}$ to the thermal plasma.

ASCOT simulationshaveshown that for NBI with ~1% ripple this torque is similar in magnitude, but opposite in direction, to the torque of injected beam neutrals. Figure 5 illustrates the collisional friction between the fast ions and the thermal plasma, T_{COL}, and the $R\boldsymbol{j}_r \times \boldsymbol{B}_p$ torque for NBI with and without ripple. While the friction is roughly unaffected by the ripple, the $R\boldsymbol{j}_r \times \boldsymbol{B}_p$ torque is strongly modified in the outer part of the plasma where it changes sign. Note that the change in the $R\boldsymbol{j}_r \times \boldsymbol{B}_p$ torque when ripple is introduced is in fact a measure of the fast ion transport since it is deduced from the radial current of fast ions, j_ϕ.

In the experiments the plasma rotation was shown to be strongly affected by the ripple, where the edge rotation changed from co- to counter-current when the ripple was increased [16]. However, the ripple-torques predicted in NBI simulations with ASCOT were in fact too small to explain the measured toroidal rotation [16-17].

SUMMARY

In preparation for TF ripple experiments in JET, Monte Carlo simulations have been performed to establish the operational boundaries that assure machine safety. The simulations show that when operating JET with enhanced ripple the ripple-induced losses could cause damage to PFC unless the NBI and ICRH power are restricted. The predictions for losses with beam ions have been shown to be in agreement with measurements; both in position and in magnitude. The simulations of the losses during ICRH were considered less reliable, in particular considering the possibility of MHD enhanced losses. The ICRH power was therefore strongly restricted and the losses were below what can be measured by the visible-light, or IR cameras. The transport of fast ions provide the thermal plasma with a toroidal $Rj_r \times B_p$-torque, where j is the return current balancing the fast ion radial current. Simulations have shown that in JET, with ~1% ripple, this torque can be of the same order as the torque of injected neutrals.

REFERENCES

[1]. A.N. Boozer, *Physics of Fluid*s **23** (1980) 2283 (1980)
[2]. P.N. Yushmanov, Reviews of plasma physics, Vol. 16
[3]. K. Tobita, et al., Nucl. Fusion **35** (1995) 1585
[4]. K. Shinohara, et al., Nucl. Fusion **43** (2003) 586
[5]. K. Tani et al., *J. Phys. Soc. Jpn* **50** 1726 (1981).

[6]. J.A. Heikkinen, et al., *Comput. Phys. Comm.* **76** (1993) 215.
[7]. J.A. Heikkinen, et al., *Nucl. Fusion* **33** (1993) 887.
[8]. J.A. Heikkinen and S.K. Sipilä, *Nucl. Fusion* **36** (1996) 1345.
[9]. J.A. Heikkinen and S.K. Sipilä, *Phys. Rev. E* 51 (1995) 1655.
[10]. J. Hedin et al., *Nuclear Fusion* **42** (2002) 527
[11]. V. Basiuk, et al., Nucl. Fusion **35** (1995) 1593
[12]. R. B. White et al, *Physics of Plasmas* **2** (1995), 2871
[13]. V. Kiptily et al., at this conference.
[14]. Gautier et al, 24th Symposium on Fusion Technology, Warsaw, Poland, 11-15 September 2006
[15]. Gautier et al, *17th Intl Conf on Plasma Surface Interactions in Fusion Devices*, Hefei Anhui, China, 22-26 May 2006
[16]. P.C. de Vries et al, submitted to *Nuclear Fusion*
[17]. V. Parail et al, *11th IAEA Technical Meeting on H-mode Physics and Transport Barriers*, Tsukuba, Japan, 26-28 September 2007.

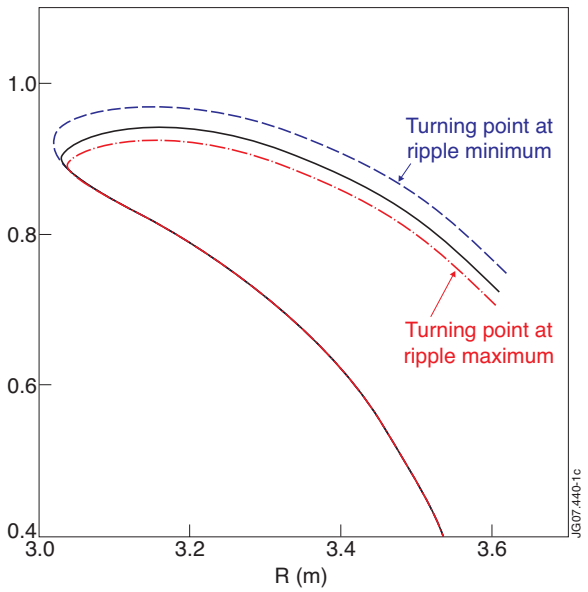

Figure 1. Cartoon of how ripple can modify a banana orbit. The orbit starts at R=3.55 m, Z=0.4 m. At the turning point the orbit is modified in a way uniquely determined by the ripple phase; near ripple maxima the turning point appears earlier (red, dotted-dash curve) than in the axisymmetric case (black, solid curve), while at ripple minima the turning point is delayed (blue, dashed curve).

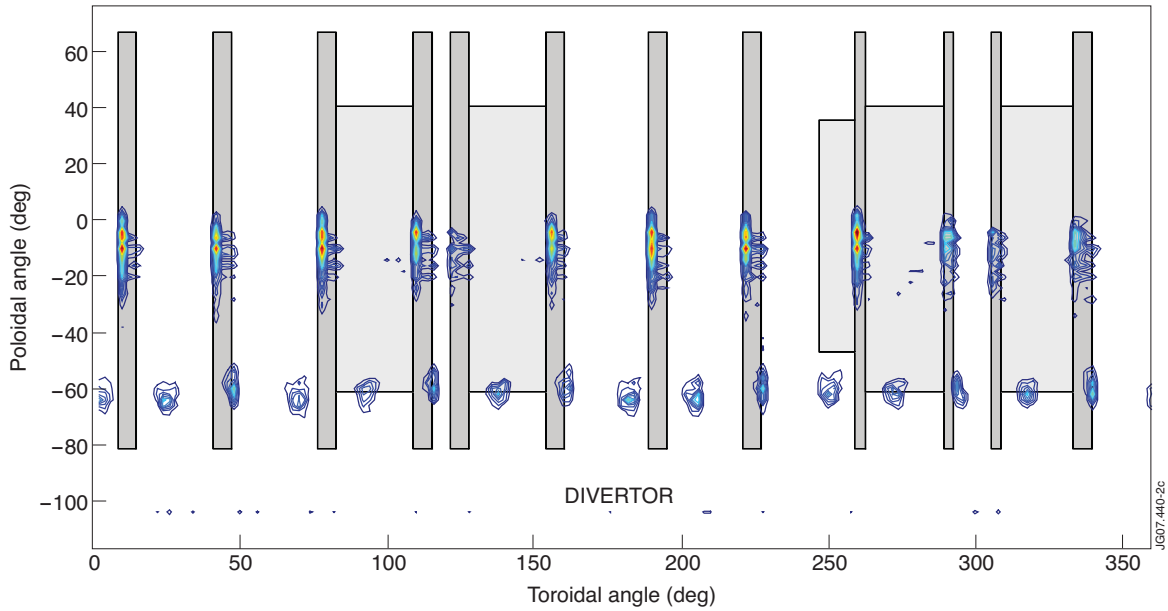

Figure 2: The colour coding indicates the heat loads to PFC calculated by OFMC for JET plasma Pulse No: 60856 with ripple amplitude 1.5%. The rectangles reaching from poloidal angles -80^o to 67^o represent the locations of the poloidal limiters, while the other rectangles represent ICRF antennas and the Lower Hybrid launcher. The resolution of the grid, on which the losses are measured in OFMC, is 2^o in both poloidal and toroidal angle. The poloidal angle 0^o is the outboard equatorial plane, while the divertor is located at around 110^o.The toroidal angle used here is increases clockwise when viewed from above.

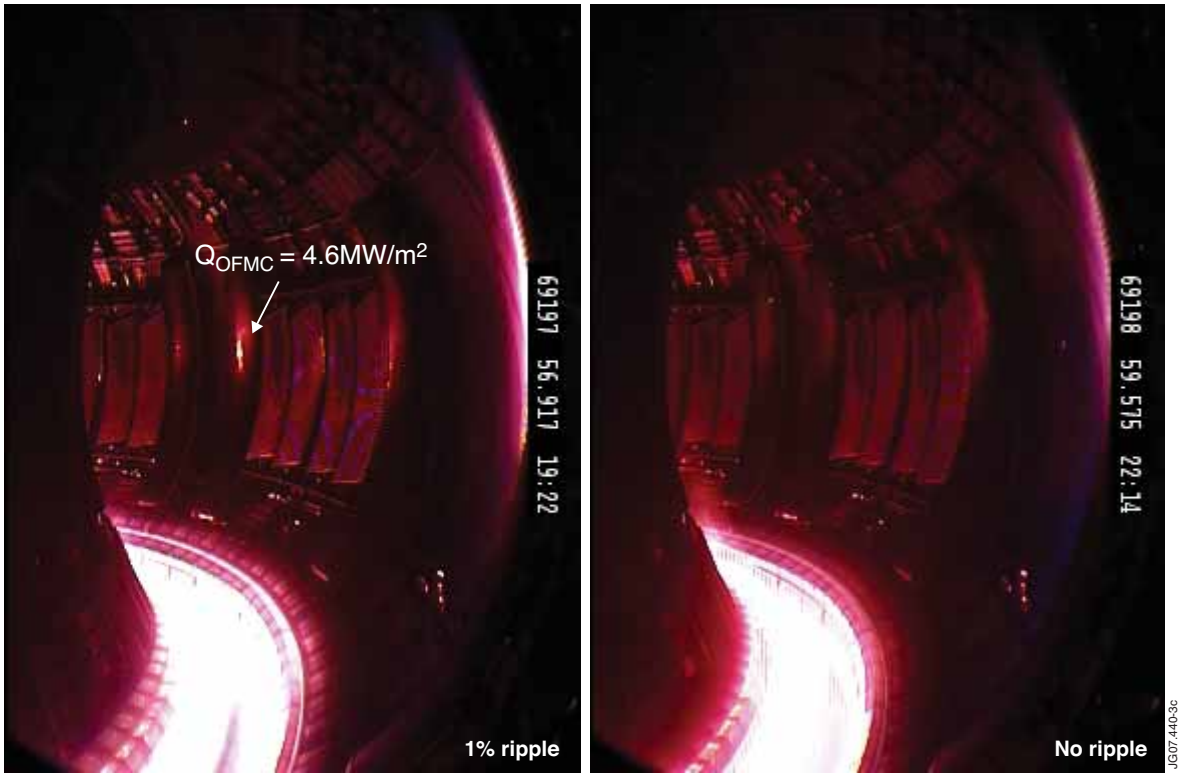

Figure 3: Observation of TF ripple induced losses (indicated by the arrow) on the poloidal limiter for a plasma with 1% ripple. Plasma with standard ripple (to the right) and similar NBI power does not show these bright spots. The pictures are taken during ELM, which illuminates many PFC (seen in red). The bright spot on the poloidal limiter, which is indicated by the arrow, is affected by the ELM cycle. In fact, the IR camera measurements show that the temperature of the limiter surface increases slowly during several seconds.

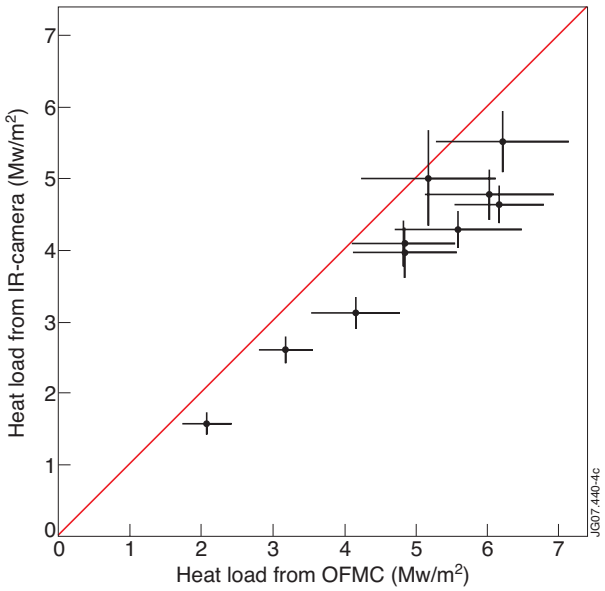

Figure 4: Comparison of the heat load calculated using the temperature rise on a poloidal limiter as measured by the IR camera and the peak power load as calculated with the OFMC code. The horizontal error-bars are derived from the statistical noise in test particle simulations and the vertical error-bars include the errors in the IR temperature measurements and in the coefficient k from Eq. (1).

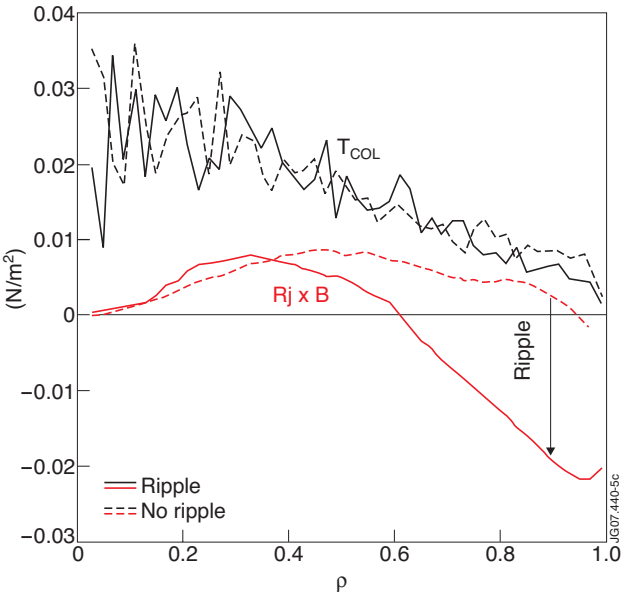

Figure 5: Fast ion torques during NBI with (solid line) and without ripple (dashed lines). The arrow illustrates the change in the Rj×B torque due to ripple transport. Note that the effect of the ripple extend deep into the plasma, from the edge to ρ ~ 0.4. Here ρ is the normalised polidal flux.